RSC Applied Polymers

ROYAL SOCIETY OF CHEMISTRY

PAPER

View Article Online
View Journal | View Issue

Cite this: *RSC Appl. Polym.*, 2025, **3**, 1258

Improving the lubricity of commercial mucins *via* conjugation with catechol-like molecules

Bernardo Miller Naranjo, [a,b] Chiara Gunnella, [a,b] Helena Wagner [a,b] and Oliver Lieleg *[a,b]

There is a range of diseases related to the insufficient lubrication of tissue surfaces. Typically, this occurs as a consequence of the reduced or incomplete production of the macromolecular key components of the respective biolubricant. Thus, developing substitute macromolecules to mitigate friction (and pain resulting thereof) in poorly lubricated joints, on the eyes, or in the oral cavity is an important task in the field of biomaterials science. To date, commercially available biomacromolecules such as hyaluronic acid (HA) and porcine gastric mucin (PGM) have mostly been in the focus of biolubrication research. However, their ability to reduce friction and surface damage generation is limited, which calls for novel approaches. Here, we create chemical modifications of commercial PGM by conjugating different catechol-like molecules (Levodopa (L-Dopa), 3,4,5-trihydroxybenzamide (THBA), or tannic acid (TA)) to the glycoprotein. Whereas solutions comprising unmodified PGMs exhibit poor lubricity, the conjugates show significantly improved surface adhesion and lubrication properties, with the TA–PGM conjugate performing the best. This particular conjugate also mitigates wear formation on PDMS and articular cartilage surfaces equally well as lab-purified porcine gastric mucin and, on hydrophilic surfaces, provides lubricity that even outperforms that of solutions comprising chemically intact, in-lab purified mucins. Our findings pave the way towards the production of a highly versatile biolubricant that can have a broad range of biomedical applications: as a biocompatible viscosupplement in osteoarthritic joints, as a lubricant additive after knee or hip implant surgery, as a component for artificial tear fluids, or for the treatment of xerostomia.

Received 22nd April 2025,
Accepted 23rd June 2025

DOI: 10.1039/d5lp00115c

rsc.li/rscapplpolym

1. Introduction

Friction reduction is essential for many interfaces in the human body to ensure that our joints and organs can fulfill their function properly. For instance, biomacromolecular lubricants are key for reducing friction in the oral cavity during speaking, chewing, and swallowing, between the cornea and the eyelid during blinking, and on articular cartilage surfaces during joint movements.[1–7] Whereas technical setups such as gears typically make use of highly viscous oils as lubricants, the composition and consistency of biological lubricants in the human body varies quite a bit: low-viscosity mucin solutions covered by a lipid film are found on ocular surfaces;[2,3] viscoelastic mucin gels protect the epithelial surfaces of the gastrointestinal tract and the cervix;[8,9] and articular joints are lubricated by the synovial fluid, which is a complex liquid containing lubricin and hyaluronic acid (HA) as key macromolecular components.[5,10–12] In all those cases, however, the absence of those biological super-lubricants leads to discomfort and disorders such as dry eye syndrome,[13] xerostomia,[14] vaginal dryness,[15] or joint pain.[16]

To improve the well-being of patients suffering from one of those conditions, scientists have been developing replacements for natural lubricants, typically by generating reconstituted solutions comprising macromolecules found in biological lubricants, mainly mucin, lubricin, and HA. However, purifying lubricin is a complex task,[11,17] and – to date – commercially purified lubricin is (to the best knowledge of the authors) not available. In contrast, purified gastric mucins are commercially available in relatively large amounts (in the scale of hundreds of grams), but tend to suffer from chemical damage inflicted during the commercial extraction process and thus show little to no lubricity compared to in-lab purified mucins. Whereas the purification process of the latter has been improved several times already,[18–20] highly functional gastric mucins are not yet available in large-scale quantities from commercial vendors.

Considering those limitations, a more feasible approach could be to use readily available (macro-) molecules and to improve their lubricity by chemically modifying them. HA is

[a]*TUM School of Engineering and Design, Department of Materials Engineering, Technical University of Munich, Boltzmannstraße 15, 85748 Garching, Germany*
[b]*Center for Protein Assemblies (CPA) and Munich Institute of Biomedical Engineering (MIBE), Technical University of Munich, Ernst-Otto-Fischer Straße 8, 85748 Garching, Germany. E-mail: oliver.lieleg@tum.de*

an example of a biomacromolecule that occurs in many locations of the human body and is highly biocompatible.[21,22] HA is commercially available in large amounts and thus is commonly used in biomedical applications such as eye drops or in viscosupplements for osteoarthritis treatment.[23–25] Recently, in two studies by Lin *et al.* and Ren *et al.*, the catechol-like molecule dopamine was conjugated to HA to improve the lubricity of HA solutions; with their approach, they observed a moderate reduction in the coefficient of friction on cartilage samples[26] and tendon,[27] respectively. Other examples of biopolymers that were suggested for the treatment of osteoarthritis include chitosan[28,29] and poly-L-lysine[30] – yet they have so far only been tested in their unmodified form. Also, lab-purified mucins have shown promise in mitigating damage formation on cartilage;[31] however, chemically modified mucins with improved lubricity have not been developed yet.

For such an approach, commercial porcine gastric mucins (even though chemically incomplete[32]) may be an interesting base material since they are well-available, have a higher molecular mass than HA, and possess a brush-like structure, which enables them to bind large amounts of water. On hydrophobic substrates, solutions comprising those commercial mucins are poor lubricants, since those mucins lack the hydrophobic termini of the polypeptide chain and therefore cannot bind to hydrophobic surfaces.[32] Previously, it was shown that such a lack of the hydrophobic termini of mucins can be somewhat compensated by chemically modifying the mucins with phenyl groups, and that this strategy can partially restore the adsorption behavior of the mucins to surfaces as well as their lubricity.[33] However, the success of this approach was limited.

Here, we aim at developing a versatile lubricant suitable for both, hydrophobic and hydrophilic substrates. We use commercial porcine gastric mucins (PGM) as a base biopolymer and draw inspiration from nature, where catechol-like molecules provide mussels and plants with the ability to attach themselves to a broad range of materials.[34–36] Accordingly, we generate conjugates of PGM with different catechol-like molecules and study the ability of those conjugates to adsorb to and desorb from PDMS surfaces. Moreover, we demonstrate the ability of those conjugate solutions to mitigate the formation of surface damage on PDMS and articular cartilage, and we show that a conjugate generated from tannic acid and PGM even outperforms the lubricity of lab-purified mucins – at least on hydrophilic substrates.

2. Materials and methods

2.1. Removing impurities from commercial mucins

Commercial PGM (Type II, Sigma Aldrich, St Louis, USA) were used as a basis for the experiments conducted in this study. To remove contaminations from those mucins (which are present in relatively high quantities in the commercial product), they were treated with a purification routine similar to the one outlined in Marczynski *et al.*[18] This procedure of removing contaminations was applied to increase the success of the conjugation steps described below. In short, 6 g of PGM were dissolved in 200 mL deionized water containing 1 M sodium chloride. Then, the solution was centrifuged for 15 min (7500 rpm; centrifuge 5430, Eppendorf, Hamburg, Germany), and the resulting pellet was discarded. The remaining supernatant was then subjected to size exclusion chromatography (GE Healthcare, Munich, Germany) employing an ÄKTA column (XK50/100, Sepharose 6FF, GE Healthcare). The fractions containing mucins were then pooled, desalinated (until the measured conductivity was below 20 μS), and concentrated using cross-flow filtration (GE Healthcare). The collected mucin solution was then frozen and lyophilized. Until further usage, the freeze-dried mucins were kept at −80 °C.

2.2. Conjugation with catechol-like molecules

The following catechol-like molecules were used to modify the commercial mucins *via* conjugation: L-3-(3,4-dihydroxyphenyl) alanine (Levodopa (L-Dopa), abcr GmbH, Karlsruhe, Germany); 3,4,5-trihydroxybenzamide (THBA, Thermo Fisher Scientific, Waltham, USA); tannic acid (TA, Sigma-Aldrich, St Louis, USA). Conjugation is conducted as follows: 15 mg *N*-(3-dimethylaminopropyl)-*N*-ethylcarbodiimide-hydrochloride (EDC, abcr GmbH, Karlsruhe, Germany), 15 mg *N*-hydroxysulfosuccinimide sodium salt (NHS, abcr GmbH), and 50 mg PGM (repurified as described above) were dissolved in 10 mL sodium phosphate buffer (SPB, pH 5.7) and incubated for 60 minutes. Then, 20 mg of a catechol-like molecule were added to the solution and incubated at ~6 °C on a rolling shaker (70 rpm, RS-TR05, Phoenix Instrument, Hannover, Germany) overnight. Any unreacted chemicals were removed by dialysis (MW cut-off: 6–8 kDa; Spectrum Labs, Waltman, USA) for 8 h. For this purpose, 20 mL of a PGM conjugate were dialyzed against ~5 L of deionized water, which was replaced once after 4 h. The resulting conjugates were freeze-dried and stored at −80 °C until further use.

2.3. UV spectroscopy

To confirm that the modification of the commercial PGM with catechol-like molecules was successful, light absorbance measurements were conducted. First, the different conjugates were dissolved in 4-(2-hydroxyethyl)-1-piperazineethanesulfonic acid buffer (HEPES, 20 mM, pH 7.0) at a concentration of 0.1% (w/v) each. In parallel, a dilution series (with the lowest concentration being 0.002% (w/v)) of the different catechol-like molecules (L-Dopa, THBA, TA) was prepared in 20 mM HEPES buffer to create a standard curve that will allow us to calculate the number of catechol-like molecules present in the conjugates. Absorbance spectra of all solutions were obtained in a wavelength range from 200 to 500 nm on a plate reader (Varioskan LUX, Thermo Fischer Scientific, Waltham, USA). These measurements were conducted on 150 μL of each solution in 96-well plates. HEPES buffer was used as a reference, and its absorbance spectrum was subtracted from all other measurements.

2.4. Adsorption experiments

To study the adsorption efficiency of different PGM-conjugates to PDMS surfaces, quartz crystal microbalance with dissipation monitoring (QCM-D) measurements were conducted on PDMS-coated gold chips using a qcell T-Q2 device (3T Analytik, Tuttlingen, Germany) as described in previous work.[32]

To generate the PDMS coating, the prepolymer was thoroughly mixed in a 10 : 1 ratio with the curing agent. The mixture was degassed in a vacuum chamber (800 mbar) and diluted in *n*-hexane (Carl Roth GmbH, Karlsruhe, Germany) to a concentration of 1% (v/v). 100 μL of this solution were slowly pipetted onto the center of a fresh and clean gold chip (3T Analytik) and evenly distributed across the surface in two steps using a spin-coater (ES-400B-6NPP/LITE, Laurell, North Wales): first, with 1000 rpm for 20 s; then, with 3000 rpm for 30 s. The coated chips were placed into a vacuum chamber for 30 min to ensure that the PDMS coating was fully degassed. Subsequently, the PDMS was baked at 80 °C for at least 4 h.

The tested different macromolecules (commercial PGM and 3 conjugates generated thereof) were dissolved at a concentration of 0.01% (w/v) in 20 mM HEPES buffer (pH 7.0). A fresh chip was used for every measurement. First, 20 mM HEPES buffer was injected at a rate of 100 μL min^{-1} for ~15 min until the chip was equilibrated and a stable, constant frequency readout was reached. Then, the macromolecule solution was injected at a rate of 100 μL min^{-1} for ~30 minutes until saturation was reached. For data analysis, the constant equilibrated frequency obtained after buffer injection was set as the zero line, and all curves were shifted along the *x*-axis so that the time point of macromolecule injection corresponds to $t = 0$. These experiments were repeated 3 times with fresh PDMS-coated chips and freshly prepared macromolecule solutions.

2.5. Dynamic light scattering measurements

To ensure that the conjugation process does not create intermolecular cross-links resulting in mucin clusters/aggregates (which would reduce the lubricity of the mucin solutions), the hydrodynamic diameter of the mucins was measured *via* dynamic light scattering (DLS) using a Litesizer 500 Zetasizer (Anton Paar, Graz, Austria). For those measurements, solutions containing 0.1% (w/v) PGM or PGM–catechol conjugates were prepared in 10 mM HEPES buffer. Then, 1000 μL of each solution were transferred into a disposable, four-clear-sided cuvette, and the hydrodynamic size of the samples was measured. For all measurements, the backscattering angle was automatically determined by the device, and the obtained signal was analyzed using an intensity-average weighting model with the assumption that the PGM and the studied conjugates have a spherical geometry.

2.6. Cytocompatibility tests

2.6.1. Leaching assay. To test the cytocompatibility of the catechol–PGM conjugates, a leaching test was conducted according to the norm ISO 10993. In detail, a leaching medium was produced, as follows: each of the catechol–PGM conjugates was exposed to UV light for disinfection (30 min, BLX E254, Vilber Lourmat GmbH, France) and then dissolved in phosphate buffered saline (PBS: 137 mM NaCl, 8.1 mM Na_2HPO_4, 1.5 mM KH_2PO_4, pH 7.4) at a concentration of 4% (w/v) solution. Then, the solution was dialyzed (MW cut-off: 1 kDa, SpectraPor 7, Carl Roth GmbH + Co. KG, Karlsruhe, Germany) against cell medium (*i.e.*, Dulbecco modified Eagle's medium (DMEM), high glucose, Sigma-Aldrich) supplemented with 10% fetal bovine serum (FBS, Sigma-Aldrich), 1% penicillin/streptomycin, 1% non-essential amino acid solution (NEAA, Sigma-Aldrich), and 1% L-glutamine (Sigma-Aldrich) for 96 hours under gentle shaking at 6 °C. For this dialysis step, the volume of the cell medium was chosen to be 10 times the volume of the sample.

In parallel, HeLa cells were cultivated from a frozen stock and maintained in cell medium at 37 °C and 5% CO_2 until confluency was reached. Then, the cells were harvested by trypsin treatment, and 5000 cells each were transferred into the wells of a 96-well plate filled with 100 μL of fresh medium. A total of six wells were prepared for each of the following groups: Control, PGM, L-Dopa–PGM, THBA–PGM, and TA–PGM. After 24 h of incubation, 50 μL of medium were removed from each well and replaced with 50 μL of the leaching medium. Then, the cells were incubated for another 24 h, and the cell viability was determined.

For this purpose, the medium was carefully withdrawn from the wells containing the cells. Afterwards, 150 μL of a 2% (v/v) water-soluble tetrazolium salt (WST-1, Roche Diagnostics GmbH, Mannheim, Germany) solution prepared in cell medium was pipetted into each well. In addition, 8 fresh wells were filled with 150 μL of this WST solution to serve as a blank for the following measurements. After 1 h of incubation, the absorbance of those WST solutions was quantified with a plate reader (Varioskan LUX, Thermo Fischer Scientific). The obtained values were treated as follows: the average absorbance was calculated for the 6 wells containing a WST solution only. Then, this average was subtracted from all measurements conducted for wells containing cells. Finally, the mean absorbance was calculated for the "Control", and this value was used to normalize the absorbance values measured for the other groups.

2.6.2. Direct exposure. HeLa cells were cultivated from a frozen stock and maintained in cell medium at 37 °C and 5% CO_2 until confluency was reached. Then, the cells were harvested by trypsin treatment, and 5000 cells each were transferred into the wells of a 96-well plate filled with 100 μL of fresh medium. A total of six wells were prepared for each of the following groups: Control, PGM, L-Dopa–PGM, THBA–PGM, and TA–PGM. After 24 h of incubation, 50 μL of medium were removed from each well and replaced with 50 μL of medium containing 1.0% (w/v) of either PGM or one of the conjugates – so that in the end, the cells experienced direct exposure to medium containing 0.5% (w/v) of either PGM or one of the conjugates. Then, the cells were incubated for another 24 h, and the cell viability was determined as described above.

2.7. Contact angle (CA) measurements

To compare the wetting behavior of coated and uncoated PDMS samples, their contact angle (CA) was determined using a commercial drop-shape analyzer device (DSA25S, Krüss GmbH, Hamburg, Germany). Uncoated samples were cleaned with 70% (v/v) ethanol and rinsed with ultrapure water; coated samples were removed from the storage buffer. A 2 μL droplet of ultrapure water was placed onto each sample, and lateral images were captured with a high-resolution built-in camera (acA1920, Basler, Ahrensburg, Germany). Each image was analyzed with the software ADVANCE (AD4021 v1.13, Krüss GmbH) using an automated fitting method ("automatic baseline", "Ellipse Tangent-1"). The static CAs were then obtained as the angle enclosed by water between the tangent to the PDMS surface and the tangent to the droplet starting at the edge of the droplet.

2.8. Rotational tribology

Tribological measurements were conducted to study the lubricating, desorption, and wear prevention performance of the different conjugates. In all cases, a commercial shear rheometer (MCR 302, Anton Paar, Graz, Austria) was equipped with a tribology unit (T-PTD 200, Anton Paar).

2.8.1. Friction measurements. A ball-on-cylinder geometry using steel spheres (∅ 12.7 mm, 1.4301, Kugel Pompel, Vienna, Austria) and polydimethylsiloxane (PDMS) cylinders was employed, as described in earlier work.[37,38] The PDMS cylinders were produced using a commercially available PDMS system (Sylgard 184, Dow Corning, Midland, MI, USA). The PDMS prepolymer was thoroughly mixed in a 10 : 1 ratio (w/w) with the curing agent and then exposed to vacuum for 1 h to remove air bubbles. After this step, the mixture was filled into a custom-made mold, cured at 80 °C overnight, and then exposed to 100 °C for 2 h to ensure that there were no unreacted residues left. The cured PDMS cylinders were removed from the mold and rinsed with 80% (v/v) ethanol and deionized water.

Friction measurements were conducted under a normal force of F_N = 6 N, which (according to Hertzian contact theory) results in an average contact pressure on PDMS of $p_0 \approx 0.31$ MPa.[39] For each measurement, 600 μL of lubricant were used: the conjugates, commercial PGM, and lab-purified mucins were each dissolved at a concentration of 0.5% (w/v) in HEPES buffer. HEPES buffer (devoid of any macromolecule) was used as reference. Logarithmic speed ramps from ~700 mm s^{-1} to 0.001 mm s^{-1} were applied, and the friction coefficient was measured at 48 different speed levels. For each condition, the measurements were conducted on n = 3 independent sample sets comprising three PDMS pins each.

To test the ability of the conjugate solutions to lubricate hydrophilic surfaces, PDMS pins were created as described above and then were treated in a plasma oven (SmartPlasma 2.0, plasma technology GmbH, Herrenberg, Germany) by exposing them to air plasma (38 W, 4 mbar, 90 s). A CA measurement was conducted after this treatment (see section 2.5 above) to ensure that the plasma-induced hydrophilization was successful (only pins with CA < 15° after plasma treatment were used for further tests). As a second hydrophilic surface, steel (1.3401, CA ~ 50°) was chosen. In this case, the maximum sliding speed was reduced to 80 mm s^{-1} to protect the measuring device from the (putatively) occurring high friction coefficients resulting from the steel-on-steel material pairing.

2.8.2. Desorption tests under shear force. Force-induced desorption tests of the different PGM-conjugates from PDMS surfaces were conducted as follows: first, passive coatings were generated by incubating PDMS pins with the respective conjugate solution for 1 h. Then, the samples were carefully placed into the tribology holder (holding 3 PDMS pins), and the steel sphere was moved for around 10 s at a sliding velocity of 10 mm s^{-1} against the pins at a normal force of F_N = 6 N as described above. CAs were measured on the samples before and after tribological treatment.

2.8.3. Wear tests. To assess the ability of different lubricants to reduce the generation of surface damage, we exposed PDMS pins and osteochondral cylinders to prolonged friction tests using steel spheres. For wear assessment on PDMS samples, the friction protocol described above was adjusted by increasing the sliding velocity over 30 min from 0.0014 mm s^{-1} to 100 mm s^{-1} following a logarithmic ramp. Then, the sliding velocity was decreased again following the same parameters, such that a whole cycle lasted one hour. In total, a given set of PDMS pins were exposed to a tribological load over a total number of 12 such cycles.

To assess wear formation/mitigation on cartilage samples, porcine knee joints were obtained from Metzgerei Boneberger GmbH (Neufahrn, Germany), and osteochondral cylinders with a diameter of 5.5 mm were drilled out of the tissue and frozen until use. Before each test, the samples were rehydrated in 20 mM HEPES buffer (pH 7.0) supplemented with 154 mM NaCl for at least 1 h. To generate wear, the osteochondral cylinders were mounted into the sample holder of the rotational tribological set-up and fixed from the side with screws.[40] Then, a tribological treatment was performed by rotating the same steel sphere described above over the cartilage samples with a constant normal force of 6 N and a constant speed of 1 mm s^{-1} over 12 hours. During this treatment, the sample holder was filled with 600 μL of a lubricant solution reconstituted in HEPES buffer supplemented with NaCl (see above). After this treatment, the cartilage samples were washed and left to dry at air to remove residual water drops located on the sample surface.

2.9. Profilometry

To assess the damage generated on the PDMS and cartilage samples upon tribological treatment, a profilometer (Keyence VK-X-1000, Tokyo, Japan) equipped with a 20× objective (CF Plan, Keyence) was employed to obtain 3dimensional images of the pin surfaces. From these images, the metrological parameter S_{tr} (which describes the isotropy of a surface; values close to 1 indicate a very isotropic surface, whereas smaller

values indicate the occurrence of structures that reduce the isotropy) was calculated according to ISO norm 25178. For PDMS samples, a total of 9 images was obtained from 3 sets of 3 PDMS pins. For cartilage wear assessment, 2 sets of 3 osteochondral cylinders each were analyzed per condition, and each sample was imaged after the tribological treatment in the central area of the sample or where features were visible. To avoid artifacts, images that showed features resulting from the sample preparation process were not considered for further analysis. Accordingly, a minimum of 38 images were analyzed for each lubricant. Prior to calculating the S_{tr} parameter, the cartilage images were corrected to remove the intrinsic curvature of the cartilage surface.

2.10. Statistical analysis

All statistical tests were conducted using the software GraphPad Prism v.10. To test for normal data distribution, a Shapiro–Wilk test was used; to test for equal variances, a two-sample *F*-test was employed. In case of normal data distribution and equal variances, a two-sample *t*-test was used to test for statistically significant differences between data sets. For data sets with normal distribution and non-equal variances, a Welch's *t*-test was employed. For data with non-normally distributed data, a Wilcoxon-Mann–Whitney test was employed. Two-tailed tests were employed to compare the results obtained from every assay presented in this manuscript, except for the data representing wear formation (where one-tailed *t*-tests were used). Differences were considered to be statistically different if a *p*-value lower than $p = 0.05$ was obtained.

3. Results and discussion

3.1. Generation and characterization of mucin conjugates with catechol-like molecules

We here target the functional carboxyl groups present in some of the most prevalent glycans (*e.g.*, sialic acid) found in PGM, and we aim at conjugating catechol-like molecules to PGM *via* carbodiimide chemistry. Such catechol-like molecules are selected since they have been reported to bind to a broad range of materials including hydrophobic and hydrophilic surfaces.[35] In detail, we choose Levodopa (L-Dopa), 3,4,5-trihydroxybenzamide (THBA), and tannic acid (TA), as depicted in Fig. 1a. This set of catechol-like molecules should be able to engage with surfaces through monovalent/divalent/trivalent, or even multivalent binding interactions – with TA offering the most complex modes of binding. We expect the primary amine groups present in L-Dopa to allow for a straightforward application of carbodiimide chemistry to generate an amide bond between these small molecules and PGM. For THBA, the coupling reaction could take place through the formation of an imide bond with the amide group of THBA. In the case of TA, neither primary amine groups nor amide groups are available; still, this molecule can be expected to form a stable conjugate with PGM *via* transesterification, *i.e.*, by reacting with one of its ester groups during the coupling reaction.

To test the success of the envisioned conjugations, we conduct light absorbance measurements (see Fig. 1b). For all conjugates, we observe an absorbance peak at a wavelength of 270–280 nm, which is absent in the absorbance spectrum of unmodified PGM. However, this wavelength range corresponds well to the absorbance peaks determined for the three different catechol-like molecules shown below. We observe that, in all cases, conjugation to PGM leads to a slight shift (~10 nm) of the absorbance peaks towards shorter wavelengths which we attribute to the slightly changed chemical environment of the catechol-like molecules when conjugated to the glycoprotein. Using the standard curves presented in Fig. 1c, we calculate the concentration of the different catechol-like molecules in the conjugate solutions and thus can estimate the degree of functionalization for the different conjugate variants.

As summarized in Fig. 1d, we achieve the highest conjugation efficiency for L-Dopa, where we find ~2500 molecules per mucin. For THBA, we find ~1000 molecules per mucin; and for TA, we find 200 molecules per mucin. The observed differences in the conjugation efficiency can be attributed to the differences in the reactivity of the functional groups present in the catechol-like molecules and the resulting coupling reactions. When converting those numbers into mass ratios, we find that the catechol-like molecules contribute 7–19% to the mass of the final conjugates, which is in a comparable range even though the molecular weight of TA is much larger than that of L-Dopa and THBA. Given that all conjugate solutions were thoroughly dialyzed before their spectroscopic analysis, we conclude that all three conjugation attempts were successful.

Owing to the presence of nucleophilic atoms in all catechol variants, it is possible that cross-linked products are generated during the conjugation process. To test this, we measured the hydrodynamic diameters of PGM and its conjugates *via* DLS experiments. However, our results (Fig. 1e) show no indication for intermolecular cross-linking or cluster formation as the observed differences in the hydrodynamic diameters are only minor and not significant.

In a next step, we test the cytocompatibility of our conjugates, which is crucial for a putative application in the biomedical field. For this purpose, we conduct cell viability tests using HeLa cells as a model cell line, which we expose to a leaching medium produced by dialyzing conjugate solution against cell medium. Our results (Fig. 1f) show cell viability values well above 80% for all conditions tested. This suggests that no cytotoxic residues are present in the conjugates.

If these conjugates are intended to be used as lubricants inside the human body, they will get in direct contact with living tissue. To study whether such direct exposure to catechol–PGM conjugates is harmful to cells, we conduct a second round of cell viability tests. Fig. 1g shows that, also here, the cell viability remains above 70% for all tested groups, which is the typical threshold for cytocompatibility. In conclusion,

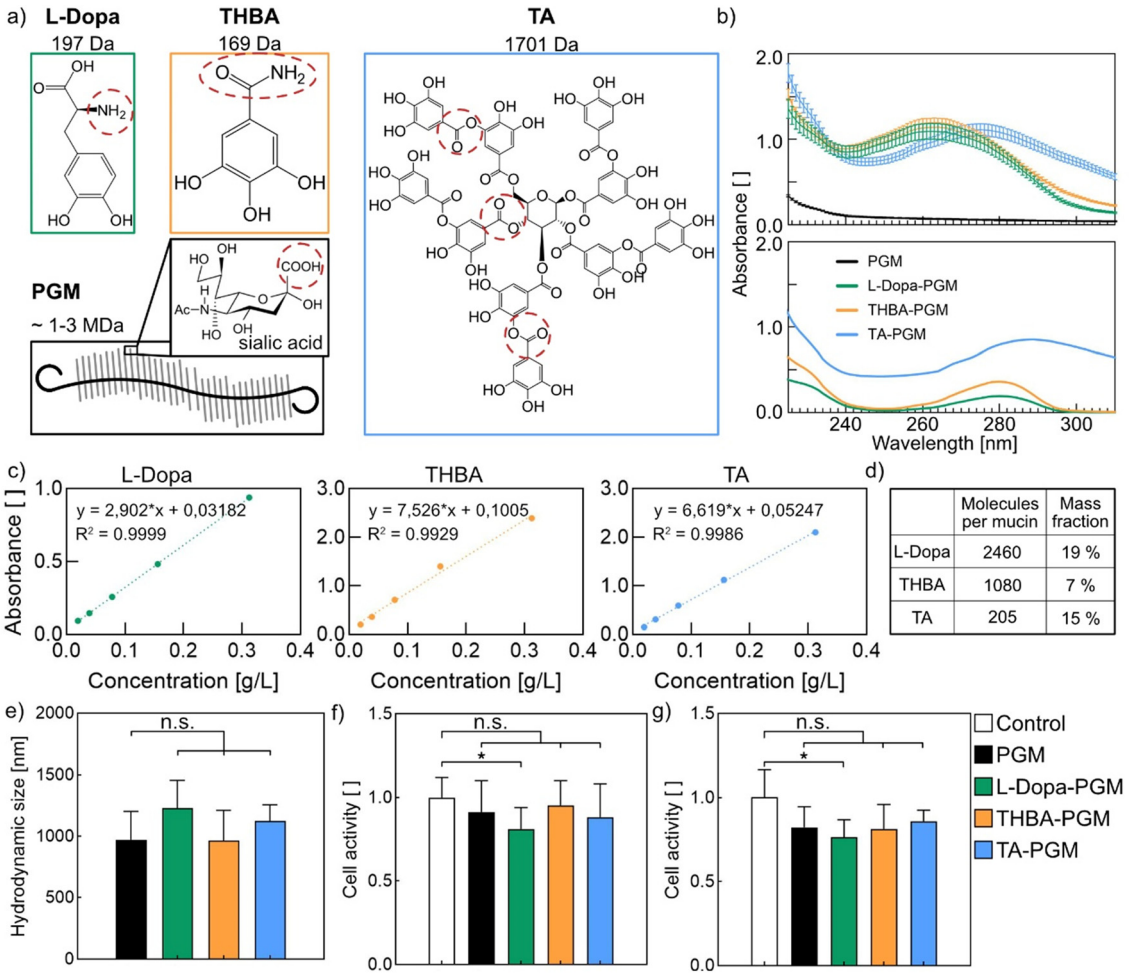

Fig. 1 Conjugation of catechol-like molecules to commercial porcine gastric mucins. (a) Chemical structures of the catechol-like molecules used in this study and a simplified model of the mucin glycoprotein. The most likely binding sites are marked with a red dotted circle. (b) Absorbance measurements were conducted on solutions comprising unmodified PGM or the different conjugates generated thereof (upper panel) as well as with solutions containing only the catechol-like molecules (lower panel). (c) Standard curves obtained from UV-VIS measurements on a dilution series of the catechol-like molecules. (d) Estimated conjugation efficiency in units of catechol-like molecules per mucin and the corresponding mass fraction of the catechol-like molecules in the conjugate. (e) Hydrodynamic diameter of PGM and its conjugates. Cytocompatibility tests conducted using a leaching medium (f) and *via* direct exposure to PGM and its conjugates (g). Data shown represents the mean, and error bars denote the standard deviation as calculated from $n \geq 5$ samples. Asterisks denote significant differences, whereas the label "n.s." denotes that no significant differences were found (based on a p-value of 0.05).

these two sets of cell tests suggest that all the conjugates studied here are cytocompatible.

3.2. Catechol conjugation enhances the ability of PGM to adsorb to hydrophobic surfaces

Native mucins exhibit hydrophobic termini that enable them to spontaneously adhere to hydrophobic surfaces such as PDMS through hydrophobic interactions. In commercial PGMs, these termini are, however, damaged or even fully absent, which is a consequence of the harsh chemical conditions during the commercial purification procedure.[32] Accordingly, commercial PGM does not adsorb well to PDMS as indicated by the rather weak frequency shift of ~80 Hz obtained from a QCM test on PDMS-coated quartz crystals using solution containing 0.01% (w/v) commercial PGM (Fig. 2a). In comparison, the frequency shift obtained for lab-purified mucins (which do contain the hydrophobic termini) at identical conditions is 4–5 times larger.[32]

Upon conjugation of a catechol-like molecule to commercial PGM, we expect the conjugate to exhibit an increased capability to bind to PDMS surfaces compared to unmodified PGM. Whereas this is not observable for the L-Dopa conjugate, the THBA-conjugate and the TA-conjugate both return larger frequency shifts of ~150 Hz and ~250 Hz, respectively. These results show that two of the catechol-like molecules tested here indeed provide the PGM-conjugate with the ability to better adsorb to hydrophobic surfaces such as PDMS than unmodified PGM itself. Moreover, the obtained data suggests that the larger number of hydroxyl groups present on THBA and TA allows for multivalent binding of those two motifs to

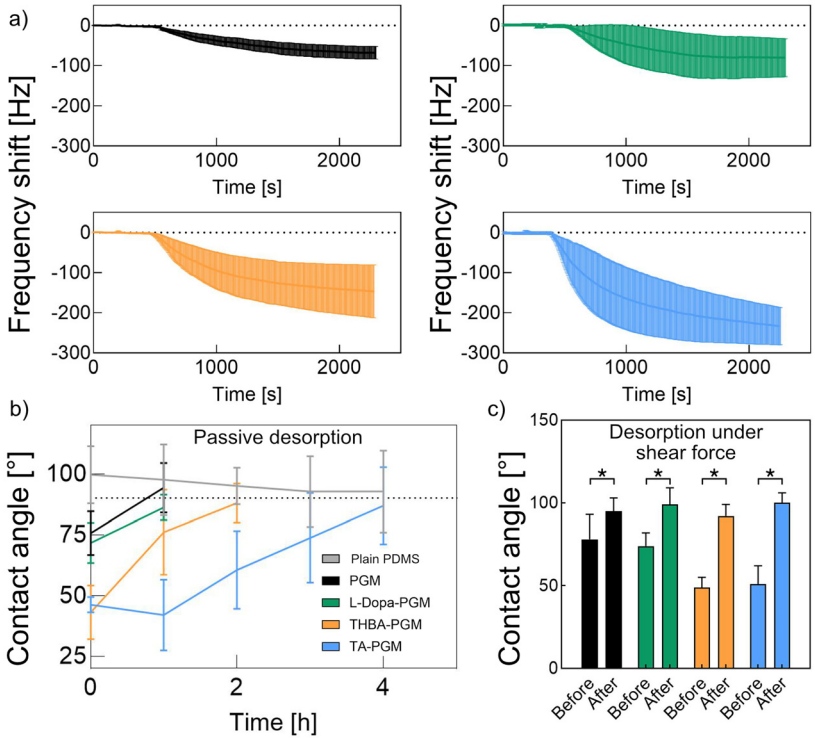

Fig. 2 Adsorption and desorption behavior of PGM and catechol–PGM conjugates to and from a hydrophobic PDMS surface. (a) Frequency shifts determined *via* QCM-D; solutions containing unmodified mucin (PGM) and conjugates generated thereof are compared. (b) Contact angle measurements to assess the ability of PGM and different PGM conjugates to spontaneously detach from a hydrophobic surface. (c) Contact angle measurements conducted on PDMS surfaces that were first passively coated with either PGM or a PGM-conjugate molecule and then exposed to shear stress. Data shown represents the mean; error bars denote the standard deviation as calculated from $n = 3$ independent samples for the QCM-D measurements and from $n \geq 5$ samples for the CA measurements. Asterisks denote significant differences between the CA values measured before and after exposure to shear force. The threshold for significance was set to $p = 0.05$.

PDMS surfaces, and that multivalent binding is helpful in conveying mucin adsorption to this substrate.

The transient bond between native mucins and hydrophobic surfaces can be broken again – either by thermal forces or upon exposure to shear stress. In fact, one of the key lubrication mechanisms mucins employ – sacrificial layer formation – relies on the cyclic process of mucins spontaneously adsorbing to a (hydrophobic) surface and desorbing again under shear.[33] As shown above, we can improve the ability of PGM to adsorb to hydrophobic surfaces through conjugation with catechol-like molecules. However, if the bond between the modified PGM and the surface were to be too strong, the conjugate might generate a permanent coating, which would be less efficient in reducing friction than a readily absorbing/desorbing mucin solution. Therefore, in a next step, we study the detachment dynamics of the different PGM conjugates. For this purpose, we generate passive coatings by incubating PDMS samples in a PBS solution containing either unmodified PGM or a catechol–PGM conjugate. We then conduct CA measurements immediately after this coating step, incubate the samples in ultrapure water, and repeat the CA measurements every hour (Fig. 2b).

Importantly, we observe that the CA obtained on PDMS is decreased by all passive mucin coatings generated here. This effect is stronger for THBA–PGM and TA–PGM (where we find a reduction of the CA from ~100° to ~50°) than for L-Dopa–PGM or unmodified PGM alone (where the CA is reduced to ~75° only). These results agree very well with our observations from the QCM-D experiments, which suggested, that THBA–PGM and TA–PGM adsorb more efficiently to PDMS (thus creating better coatings) than L-Dopa–PGM or unmodified PGM. Interestingly, this hydrophilizing effect disappears after 1 h for PGM and L-Dopa–PGM, after 2 h for THBA–PGM, and after 4 h for TA–PGM. Based on these results, we conclude that the adhesion strength of all three conjugates is weak enough to allow for a spontaneous desorption driven by thermal energy.

Of course, during exposure to tribological shear forces, a desorption time of 4 h would be much too large to allow for an efficient sacrificial layer mechanism. Thus, in a next step, we ask if shear forces generated by tribological load can quickly remove surface-adsorbed catechol–mucin conjugates from their substrate. Also here, we generate passive coatings on PDMS samples, measure the initial CA brought about by the coatings, and then expose the coatings to shear forces using a commercial rheometer equipped with a tribology unit. After a shear stress application for ~10 s, we repeat the CA measurements and observe that all samples have recovered their initial

hydrophobicity (Fig. 2c). In other words, we can conclude that all passive coatings have (almost) fully been detached from the PDMS substrate upon exposure to tribological shear stress.

3.3. Catechol conjugation improves the lubricity and wear prevention abilities of PGM

Having demonstrated that conjugation of catechol-like molecules to PGM can improve the adsorption of the glycoprotein to PDMS while maintaining its ability to desorb, it is reasonable to assume that solutions containing these conjugates will be more lubricious than solutions made from PGM alone – as this cyclic binding/unbinding process of mucins to and from surfaces is required for the lubricating mechanism known as 'sacrificial layer formation' to occur. To test this hypothesis, we conduct friction measurements over a broad spectrum of sliding velocities (0.01–750 mm s^{-1}) and employ a steel-on-PDMS material pairing as typical for biotribological studies.[41–44]

As summarized in Fig. 3a, a 0.5% (w/v) solution of unmodified PGM prepared in 20 mM HEPES buffer has a similarly low lubricity as pure HEPES buffer devoid of any mucins: in both cases, we find very high friction coefficients close to one over a broad range of sliding speeds. In contrast, a 0.5% (w/v) solution containing lab-purified porcine gastric mucins (MUC5AC) provides excellent lubricity with friction coefficients of 0.01 and below. This underscores the outstanding ability of chemically intact mucins to reduce friction in the boundary and mixed lubrication regime. Only at very high sliding velocities (above ~200 mm s^{-1}), the three lubricants perform similarly. Here, in the hydrodynamic lubrication regime, differences between lubricants are mostly dictated by differences in their viscosity;[45] and as shown in Fig. 3b, all solutions tested here exhibit virtually identical viscosities at high shear rates.

For solutions containing 0.5% (w/v) L-Dopa–PGM, the obtained friction curve is very similar to the one obtained for unmodified PGM, which agrees with the adsorption data discussed above. However, we find a slight, yet significant reduction in friction for solutions containing 0.5% (w/v) THBA–PGM and a strong reduction for solutions containing 0.5% (w/v) TA–PGM; for the latter, we observe friction coefficients around ~0.1, which is a clear improvement compared to the result obtained for unmodified PGM – but still one order of magnitude away from the excellent result obtained with lab-purified mucin.

At low sliding speeds (corresponding to low shear rates), those TA–PGM solutions exhibit a 100-fold higher viscosity

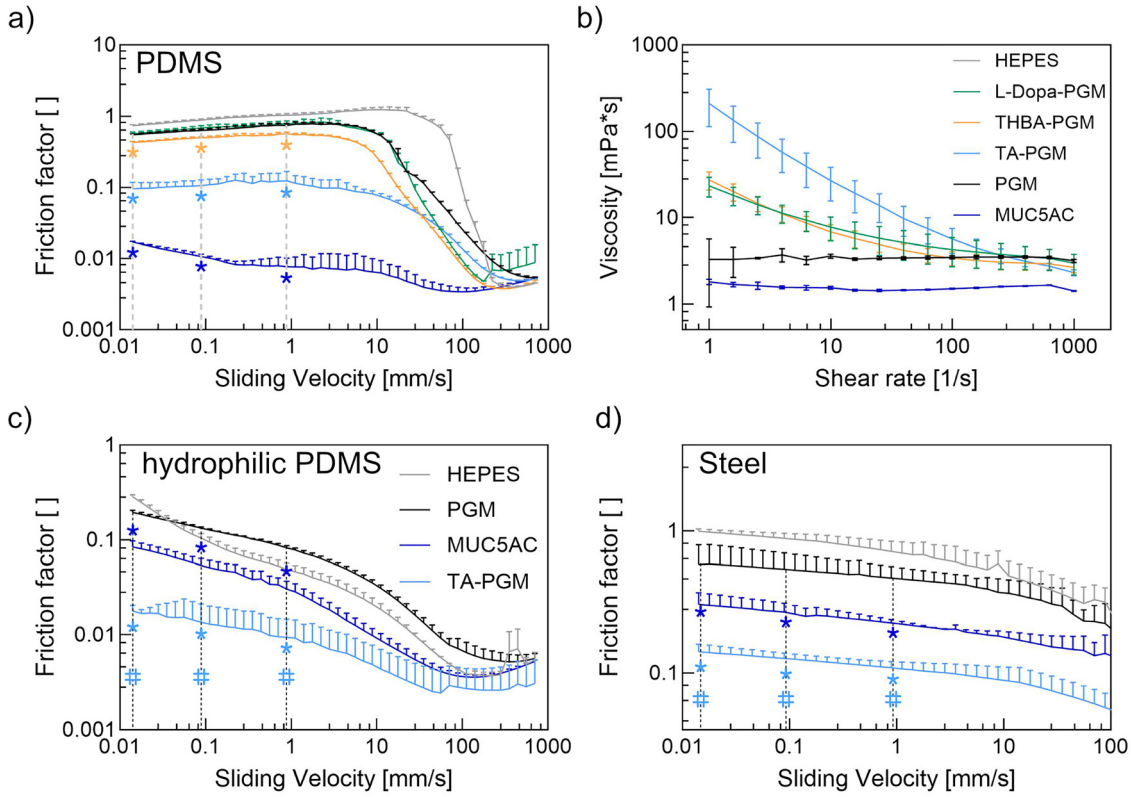

Fig. 3 Lubricity and viscosity of solutions comprising either PGM or catechol–PGM conjugates. (a) Friction curves obtained using a steel-on-PDMS material pairing. (b) Viscosities of the different solutions. (c and d) Friction factor measurements conducted on hydrophilic surfaces, *i.e.* hydrophilized PDMS and steel. In all cases, results obtained for pure HEPES buffer and for solutions comprising lab-purified mucin MUC5AC are shown for comparison. Data shown represents the mean; error bars denote the standard deviation as calculated from $n = 3$ independent samples. In subfigures (a), (c), and (d), asterisks denote significant differences compared to PGM, whereas rhombi denote significant differences compared to lab-purified MUC5AC. In either case, the threshold for significance was set to $p = 0.05$.

than solutions containing unmodified PGM. However, according to Stribeck's theory, a high-viscosity lubricant would merely shift the friction curve towards slower velocities thus reducing the width of the boundary lubrication regime. Importantly, the solution containing lab-purified MUC5AC has the lowest viscosity among all mucin solutions tested here but nevertheless very clearly outperforms all other lubricants in terms of friction reduction. In other words, for the lubricating effect brought about by TA–PGM solutions at low sliding velocities, their higher viscosity compared to solutions containing unmodified PGM is not relevant.

Based on the results discussed so far, we conclude that TA–PGM is the most promising conjugate to conduct further tests with. Indeed, a good lubricant should not only reduce friction but should also be able to prevent the formation of surface damage/wear induced by mechanical forces. To test if solutions containing the TA–PGM conjugate have wear-preventing capabilities, we conduct extended friction measurements on PDMS samples over a time span of 12 hours, and we compare the topography of the PDMS surfaces before and after this tribological treatment. When employing only buffer as a lubricant, such topographical images (see Fig. 4a) indicate damage formation on the PDMS samples in response to tribological stress: we observe parallel grooves at those locations, where the steel sphere was in contact with the PDMS surface. A similar, yet less pronounced damage pattern occurs when using solutions containing unmodified PGM as a lubricant. In contrast, those damage patterns are strongly reduced (or even fully

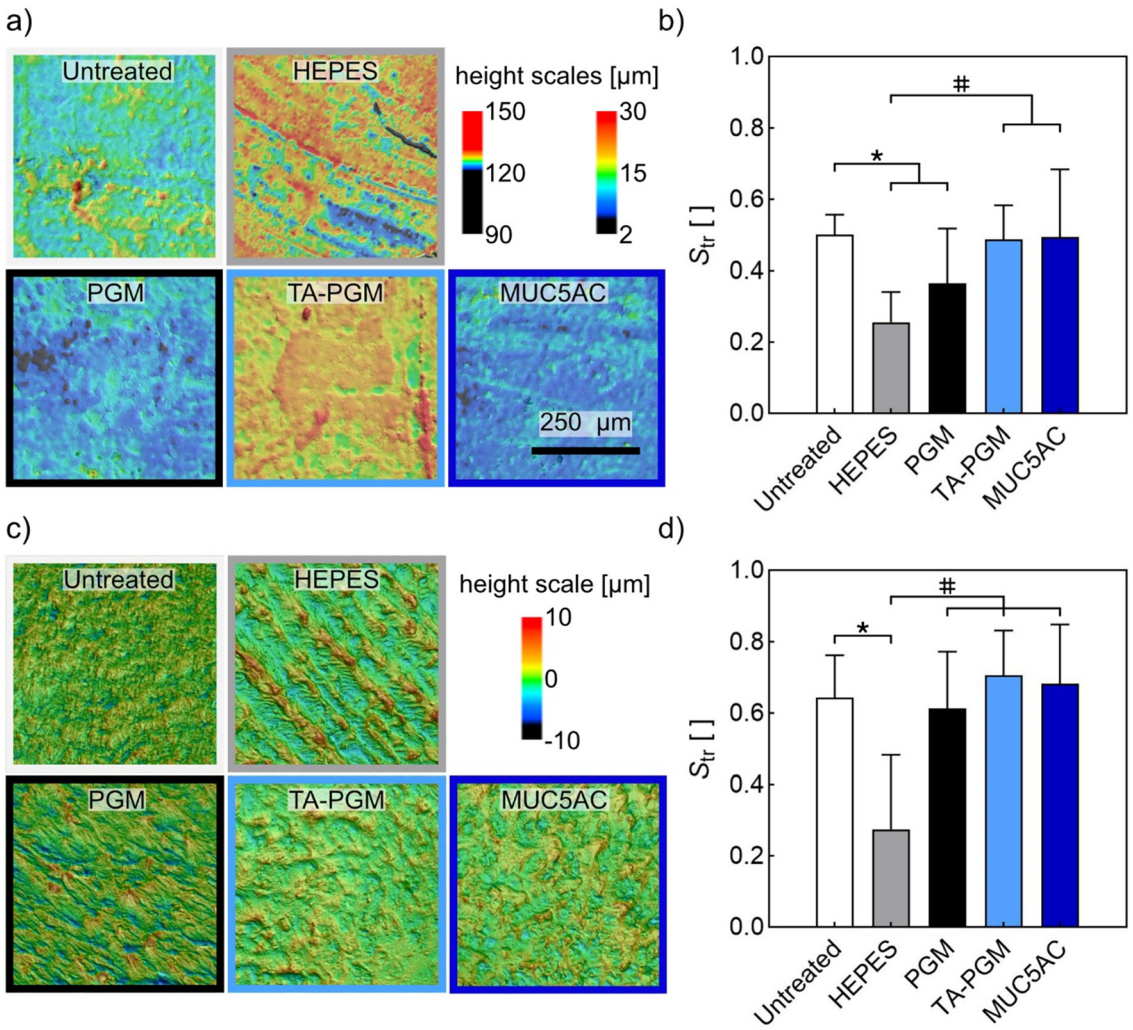

Fig. 4 Wear analysis of PDMS and cartilage samples after tribological treatment in the presence of different lubricants. (a) Topographical images of the surface of the PDMS pins before (untreated) and after tribological treatment. The left height scale applies to the HEPES-treated sample, and the right height scale applies to all other samples. (b) Surface parameter S_{tr} as determined for PDMS pins before and after tribological treatment. (c) Topographical images of the surface of cartilage samples before (untreated) and after tribological treatment. (d) Surface parameter S_{tr} as determined for cartilages samples before and after tribological treatment. Data shown represents the mean; error bars denote the standard deviation as calculated from $n \geq 9$ independent samples. Asterisks denote significant differences compared to untreated samples, rhombi denote significant differences compared to samples treated using HEPES buffer as a lubricant. The threshold for significance was set to $p = 0.05$. The scale bar in (a) represents 250 µm and applies to all images in (a) and (c).

absent) when using solutions containing either lab-purified MUC5AC or TA–PGM as a lubricant.

To quantify this impression, we calculate the metrological surface parameter S_{tr} from the different topographical images. This parameter describes the isotropy of a surface (see Methods) and is selected since, in previous studies, it was found that it can sensitively report linear grooves as we detect them here on the PDMS samples.[31] And indeed, as shown in Fig. 4b, this S_{tr} parameter is significantly altered after tribological treatment when using either HEPES buffer or a solution comprising unmodified PGM; in other words, it correctly reports the surface damage detected *via* visual inspection. In contrast, when comparing samples treated with HEPES buffer to samples treated with solutions containing either TA–PGM or lab-purified MUC5AC, the surface isotropy of samples from the latter two groups is significantly higher, which demonstrates a mitigation of wear formation. Importantly, there is no significant difference between untreated samples and samples treated with solutions comprising either MUC5AC or TA–PGM, which underscores that those two lubricants keep the PDMS surfaces very well intact.

Of course, from the point of view of a putative biomedical application, PDMS samples are not really relevant. Thus, we aim at confirming the wear-mitigating abilities of the TA–PGM conjugate by conducting wear tests on articular cartilage samples. Similar to our observations made on PDMS, also here, we find that the surface of cartilage samples lubricated with HEPES buffer only exhibit a pattern of parallel grooves (Fig. 4c). In contrast, we do not find this wear feature on cartilage samples treated in the presence of solutions containing either PGM, TA–PGM, or MUC5AC. A quantification of the corresponding topographical images by calculating the S_{tr} parameter (Fig. 4d) confirms this assessment: compared to untreated cartilage samples, this value is only significantly reduced for the group treated with HEPES buffer; this shows that, in this case, all solutions containing a mucin variant (be it PGM, TA–PGM, or MUC5AC) successfully protect the cartilage surface from damage formation.

In a final step, we conduct tribological measurements on hydrophilic surfaces. Those additional tests are motivated by the ability of catechols to bind to a broad range of surfaces including hydrophobic and hydrophilic materials. With this realization in mind, the TA–PGM conjugate should also perform well on hydrophilic surfaces. And indeed, as shown in Fig. 3c and d, TA–PGM solutions not only significantly reduce the friction factor in a steel-on-hydrophilized PDMS and a steel-on-steel material pairing when compared to solutions containing unmodified PGM – they even significantly outperform solutions containing lab-purified MUC5AC. We interpret this astonishing result as follows: MUC5AC can interact with hydrophilic surfaces through either hydrogen bonds (mediated by the large number of glycan chains) and/or electrostatic interactions (if the surface is charged), but the efficiency of those interactions is limited. Catechol-based interactions are, however, very versatile and can – at least for a multivalent conjugate such as TA–PGM – be very efficient in conveying binding to both, hydrophobic and hydrophilic substrates. Thus, by conjugating tannic acid to chemically damaged PGM, it is not only possible to restore (to some extent) the natural lubricity of the glycoprotein on hydrophobic surfaces, but solutions generated from the conjugate seem to be even more versatile lubricants than solutions containing carefully purified, intact mucins.

4. Summary and outlook

Here, we demonstrated how a simple modification of commercial mucins (*i.e.*, a conjugation with catechol-like molecules such as THBA and TA) improves the absorption and lubrication properties of the mucins. Importantly, on hydrophilic surfaces, the lubricity brought about by the TA–PGM variant even outperforms results obtained with carefully purified, native porcine gastric mucins. This is astonishing as, to date, solutions comprising such intact mucins have been the gold standard for a versatile macromolecular biolubricant.

These results are very promising, as they allow us to tackle two major long-existing challenges: first, commercial PGM is comparably inexpensive, but it also lacks the adhesive and lubricating properties of native gastric mucin. The rather simple conjugation with TA conducted here is an inexpensive modification that entails a (partial) re-functionalization of the damaged mucins. Second, a lubricant that successfully reduces friction and surface damage generation on a broad range of surfaces can have very interesting applications in medical settings: prostheses used for joint replacements are often produced from steel, and a bio-based lubricant that interacts well with this inorganic material and cartilage alike could improve the long-term performance of hip or knee implants, for instance by reducing the problem of debris generation from the implant and the subsequent inflammation response of the body.[46] Thus, future studies should explore the long-term behavior of biomedically relevant material pairings in terms of lubricity and wear.

Author contributions

OL, BMN, and CG designed the experiments. HW, CG, and BMN acquired and analyzed the data. The manuscript was written by CG, BMN, and OL. All authors gave approval to the final version of the manuscript.

Conflicts of interest

The authors declare no conflict of interest.

Data availability

Data will be made available upon request from the authors.

Acknowledgements

This study was supported by the German Research Foundation (DFG) *via* grant LI-1902/15-1. The authors thank the butcher shop Metzgerei Boneberger GmbH for kindly providing the cartilage used in this paper.

References

1 A. Sarkar, E. Andablo-Reyes, M. Bryant, D. Dowson and A. Neville, *Curr. Opin. Colloid Interface Sci.*, 2019, **39**, 61–75.
2 I. Cher, *Ocul. Surf.*, 2008, **6**, 79–86.
3 C. W. Lievens and E. Rayborn, *Clin. Ophthalmol.*, 2022, 973–980.
4 T. A. Schmidt, D. A. Sullivan, E. Knop, S. M. Richards, N. Knop, S. Liu, A. Sahin, R. R. Darabad, S. Morrison and W. R. Kam, *JAMA Ophthalmol.*, 2013, **131**, 766–776.
5 T. Schmidt, B. Schumacher, G. Nugent, N. Gastelum and R. Sah, *Trans. 51st Annu. Meet. Orthop. Res. Soc.*, 2005, **30**, 900.
6 A. R. Jones, J. P. Gleghorn, C. E. Hughes, L. J. Fitz, R. Zollner, S. D. Wainwright, B. Caterson, E. A. Morris, L. J. Bonassar and C. R. Flannery, *J. Orthop. Res.*, 2007, **25**, 283–292.
7 A. M. S. Plath, P. H. C. de Lima, A. Amicone, E. G. Bissacco, M. Mosayebi, S. B. R. Berton and S. J. Ferguson, *Biomater. Adv.*, 2024, 214129.
8 M. Curlin and D. Bursac, *Front. Biosci.*, 2013, **5**, 507–515.
9 M. E. Johansson, H. Sjövall and G. C. Hansson, *Nat. Rev. Gastroenterol. Hepatol.*, 2013, **10**, 352–361.
10 R. Crockett, *Tribol. Lett.*, 2009, **35**, 77–84.
11 T. A. Schmidt, N. S. Gastelum, Q. T. Nguyen, B. L. Schumacher and R. L. Sah, *Arthritis Rheum.*, 2007, **56**, 882–891.
12 S. Jahn, J. Seror and J. Klein, *Annu. Rev. Biomed. Eng.*, 2016, **18**, 235–258.
13 M. Kim, Y. S. Chun and K. W. Kim, *Sci. Rep.*, 2022, **12**, 2172.
14 K. Delli, F. K. Spijkervet, F. G. Kroese, H. Bootsma and A. Vissink, *Monogr. Oral Sci.*, 2014, **24**, 109–125.
15 V. Goncharenko, R. Bubnov, J. Polivka, P. Zubor, K. Biringer, T. Bielik, W. Kuhn and O. Golubnitschaja, *EPMA J.*, 2019, **10**, 73–79.
16 N. Arden and M. C. Nevitt, *Best Pract. Res., Clin. Rheumatol.*, 2006, **20**, 3–25.
17 G. D. Jay, D. A. Harris and C.-J. Cha, *Glycoconjugate J.*, 2001, **18**, 807–815.
18 M. Marczynski, C. A. Rickert, T. Fuhrmann and O. Lieleg, *Sep. Purif. Technol.*, 2022, **294**, 121209.
19 J. P. Celli, B. S. Turner, N. H. Afdhal, R. H. Ewoldt, G. H. McKinley, R. Bansil and S. Erramilli, *Biomacromolecules*, 2007, **8**, 1580–1586.
20 V. J. Schömig, B. T. Käsdorf, C. Scholz, K. Bidmon, O. Lieleg and S. Berensmeier, *R. Soc. Chem. Adv.*, 2016, **6**, 44932–44943.
21 H. Yuan, P. Xiao, B. Sarmento, G. Chen and W. Cui, *Adv. Funct. Mater.*, 2024, **34**, 2406668.
22 G. Kogan, L. Šoltés, R. Stern and P. Gemeiner, *Biotechnol. Lett.*, 2007, **29**, 17–25.
23 X. Han, S. Scialla, E. Limiti, E. T. Davis, M. Trombetta, A. Rainer, S. W. Jones, E. Mauri and Z. J. Zhang, *Biomater. Adv.*, 2024, **163**, 213956.
24 H. Zhang, J. Faber, S. Budday, Q. Gao, S. Kuth, K. Zheng and A. R. Boccaccini, *Biomater. Adv.*, 2025, **167**, 214089.
25 L. Hynnekleiv, M. Magno, E. Moschowits, K. A. Tønseth, J. Vehof and T. P. Utheim, *Acta Ophthalmol.*, 2024, **102**, 25–37.
26 K. Ren, H. Wan, H. J. Kaper and P. K. Sharma, *J. Colloid Interface Sci.*, 2022, **619**, 207–218.
27 W. Lin, R. Mashiah, J. Seror, A. Kadar, O. Dolkart, T. Pritsch, R. Goldberg and J. Klein, *Acta Biomater.*, 2019, **83**, 314–321.
28 F. Oprenyeszk, M. Chausson, V. Maquet, J.-E. Dubuc and Y. Henrotin, *Osteoarthr. Cartil.*, 2013, **21**, 1099–1107.
29 F. Comblain, G. Rocasalbas, S. Gauthier and Y. Henrotin, *Bio-Med. Mater. Eng.*, 2017, **28**, S209–S215.
30 J. Lin, W. Hu, T. Gao, B. Bao, X. Li, T. Huang, Y. Sun, J. Shen, H. Xu and K. Zhu, *Chem. Eng. J.*, 2022, **430**, 133018.
31 K. Boettcher, B. Winkeljann, T. A. Schmidt and O. Lieleg, *Biotribology*, 2017, **12**, 43–51.
32 M. Marczynski, K. Jiang, M. Blakeley, V. Srivastava, F. Vilaplana, T. Crouzier and O. Lieleg, *Biomacromolecules*, 2021, **22**, 1600–1613.
33 B. T. Käsdorf, F. Weber, G. Petrou, V. Srivastava, T. Crouzier and O. Lieleg, *Biomacromolecules*, 2017, **18**, 2454–2462.
34 P. Das and M. Reches, *Nanoscale*, 2016, **8**, 15309–15316.
35 J. Saiz-Poseu, J. Mancebo-Aracil, F. Nador, F. Busqué and D. Ruiz-Molina, *Angew. Chem., Int. Ed.*, 2019, **58**, 696–714.
36 T. M. Lutz, C. Kimna, A. Casini and O. Lieleg, *Mater. Today Bio*, 2022, **13**, 100203.
37 T. Crouzier, K. Boettcher, A. R. Geonnotti, N. L. Kavanaugh, J. B. Hirsch, K. Ribbeck and O. Lieleg, *Adv. Mater. Interfaces*, 2015, **2**, 1500308.
38 M. Biegler, J. Delius, B. T. Käsdorf, T. Hofmann and O. Lieleg, *Biotribology*, 2016, **6**, 12–20.
39 B. Winkeljann, P. M. A. Leipold and O. Lieleg, *Adv. Mater. Interfaces*, 2019, **6**, 1900366.
40 K. Boettcher, S. Grumbein, U. Winkler, J. Nachtsheim and O. Lieleg, *Rev. Sci. Instrum.*, 2014, **85**, 093903.
41 M.-A. van Stee, E. de Hoog and F. van de Velde, *Biotribology*, 2017, **11**, 84–91.
42 A. Sarkar and E. M. Krop, *Curr. Opin. Food Sci.*, 2019, **27**, 64–73.
43 N. Brossard, H. Cai, F. Osorio, E. Bordeu and J. Chen, *J. Texture Stud.*, 2016, **47**, 392–402.
44 J. Song, B. Winkeljann and O. Lieleg, *ACS Appl. Bio Mater.*, 2019, **2**, 3448–3457.
45 R. Stribeck, *Z. Vereines Dtsch. Ing.*, 1902, **46**, 1341–1348, 1432–1438, 1463–1470.
46 S. Jaiswal, A. Dubey, S. Ghosh, M. Abhishek, P. Roy, D. Lahiri and A. K. Das, *Biomater. Adv.*, 2023, **147**, 213347.